Articles

Effects of Dendrimer Generation on Site Isolation of Core Moieties: Electrochemical and Fluorescence Quenching Studies with Metalloporphyrin Core Dendrimers

Keith W. Pollak,[†] Jeffrey W. Leon,[‡] Jean M. J. Fréchet,*[,†] Michael Maskus,[‡] and Héctor D. Abruña[‡]

Department of Chemistry, University of California, Berkeley, California 94720-1460, and Department of Chemistry, Baker Laboratory, Cornell University, Ithaca, New York 14853-1301

Received May 2, 1997. Revised Manuscript Received October 2, 1997[⊗]

The ability of a dendritic shell to afford site isolation to a porphyrin core was evaluated using electron-transfer experiments with a series of porphyrin-core dendrimers. Cyclic voltammograms show that surrounding a porphyrin site with even a small generation ($G \sim 2$) dendrimer can significantly lower the rate of interfacial electron transfer, ostensibly by decreasing the proximity of the porphyrin core to the electrode surface. This inhibition of electron transfer is more pronounced when larger generation dendrimers are employed. While a significant measure of site isolation is achieved with respect to an electrode surface, no hindrance to penetration of a small molecule is afforded by the dendritic shell surrounding the porphyrin core, an encouraging result if dendrimers are to be designed as macromolecular hosts with a functioning catalyst at the core. Stern−Volmer analysis was used to investigate the accessibility of a small molecule, benzylviologen, to the porphyrin core. For generations 1−3, the dendritic structure surrounding the porphyrin core does not significantly inhibit the ability of the viologen to quench the fluorescence of the metalloporphyrin. When the porphyrin is surrounded by fourth-generation dendrons, a slight rate enhancement was observed with quenching being 33% faster. Absorption and fluorescence spectroscopies of solutions of the porphyrin-core dendrimers also suggest that the dendrimeric surroundings do not interfere electrochemically or photophysically with the porphyrin core. The characteristic wavelengths of absorption and emission of the porphyrin moiety did not change as the dendrimer generation was increased, indicating that the dendritic substituents do not appear to significantly affect the electrochemical and photophysical nature of the metalloporphyrin core.

Introduction

Syntheses of bulky or sterically hindered metalloporphyrins with specific architectures have been developed for various biomimetic systems. Three of the more common natural archetypes are chlorophyll, globulin, and metal-containing enzymes. The light-harvesting and electron-transfer properties of chlorophyll have been modeled by synthetic tetraarylmetalloporphyrins with electron-donating or electron-withdrawing substituents.[1] Other metalloporphyrins, with one sterically obstructed face, have been synthesized to model proteins such as hemoglobin and myoglobin, which bind and transport molecular oxygen.[2] However, the most common purpose for synthesizing porphyrins with defined architecture has been to model natural oxidation catalysts such as the cytochromes.[3,4]

Some of the latest models have involved embedding porphyrins at the core of a dendrimer. The resulting molecules can resemble their natural analogues in dimension and functionality.[5] Through well-defined design, a dendrimer engulfing a porphyrin core might begin to mimic a natural catalyst.

* Address correspondence to this author at the University of California, Berkeley.
[†] University of California.
[‡] Cornell University.
[⊗] Abstract published in *Advance ACS Abstracts,* December 15, 1997.

(1) (a) Seely, G. R. *Photochem. Photobiol.* **1978**, *2*, 107. (b) Wagner, R.; Ruffing, J.; Breakwell, B.; Lindsey, J. *Tetrahedron. Lett.* **1991**, *32*, 1703. (c) Wagner, R.; Lindsey, J.; Turowska-Tyrk, I.; Scheidt, W. *Tetrahedron* **1994**, *50*, 11097. (d) Lindsey, J. S.; Prathapan, S; Johnson, T. E.; Wagner, R. W. *Tetrahedron*. **1994**, *50*, 8941.
(2) Collman, J.; Brauman, J.; Fitzgerald, J.; Hampton, P.; Naruta, Y.; Sparapany, J.; Ibers, J. *J. Am. Chem. Soc.* **1988**, *110*, 3477.
(3) Quici, S.; Banfi, S.; Pozzi, G. *Gazz. Chim. Ital.* **1993**, *123*, 597. Quintana, C.; Assink, R.; Shelnutt, *J. Inorg. Chem*. **1989**, *28* 3421.
(4) (a) Montanari, F.; Casella, L. *Metalloporphyrins Catalyzed Oxidations*; Kluwer Academic Press: Boston, 1994. (b) Sheldon, R. A. *Metalloporphyrins in Catalytic Oxidations*; Dekker: New York, 1994.

S0897-4756(97)00312-8 CCC: $15.00
Published on Web 01/19/1998

Nanoenvironment within Dendrimers. Dendrimers[6,7] have been shown to exhibit dimensions and host/guest capabilities that resemble those of some naturally occurring catalytic species.[7] As their sizes increase, convergent polyether dendrimers (of the fourth generation and higher) have been shown to assume a globular conformation.[6,8] Because the dendrimer molecules can easily adopt globular conformations providing an "inner" volume, these and other dendrimers may be used to solubilize a variety of organic compounds.[9−11] In addition, if their chain ends are appropriately designed or modified, the dendrimers can behave as water-soluble, unimolecular micelles.[10] Hydrophobic[10c] and other interactions are used to solvate the guest molecules within the water-soluble dendrimers. Meijer and co-workers[11] have described both the ability of small molecules to penetrate a dendrimer and their trapping through a modification of the outer dendritic shell. More recently, convergent benzyl ether dendrimers have been shown to provide effective site isolation for metal ions[12a] and clusters[12b] or a special nanoenvironment in which reactions that normally do not proceed satisfactorily in solution may be performed. For example, the focal point of a convergent dendrimer may be used to initiate the anionic polymerization of caprolactone.[13] A high molecular weight polymer is obtained because "back-biting" is prevented as a result of the unique nanoenvironment that is provided for the propagating end within the relatively polar "interior" of the dendrimer. Similarly, the use of solvatochromic probes[14] has shown that a unique nanoenvironment may exist within large dendrimers. The synergy of these unique properties could lead to efficient and robust biomimetic dendritic catalysts.

In this report, we present studies of the electrochemical behavior of four porphyrin-core dendrimers. Each porphyrin ring is metalated with zinc and meso-substituted with a benzyl ether dendrimer varying in size, from generation one to generation four (Figure 1). The porphyrin ring embedded at the core of the dendrimer was used as an electrochemically active moiety to study the accessibility of the dendrimer core through electron-transfer reactions between an electron donor and an electron acceptor, which can probe the physical environment encountered by these molecules.[15] In general, if the donor/acceptor pair is physically separated, then the rate of electron transfer must decrease. Turro et al. have demonstrated[16] the "blocking ability" of dendrimers by measuring the electron transfer between photoexcited $[Ru(bpy)_3^{2+}]^*$ and methylviologen, an electron donor and an acceptor respectively, in a solution that also contained carboxylate-terminated PAMAM dendrimer. They concluded that both the donor and acceptor rest on the dendrimer surface, which acts to separate them and therefore decreases the rate of electron transfer. The larger the dendrimer, the larger the surface and the distance between the donor and acceptor; therefore the rate of electron transfer decreases.

To date, few data have been published regarding the effect of a dendrimer surrounding an electrochemically active site, potentially a catalyst. Physical measurements on dendrimers with a compact structure suggest that high-generation dendrimers ($G \geq 3$) encapsulate the core.[7,8,12,14] In the case of the porphyrin-core dendrimers,[5] the large size of the core makes such an occurrence unlikely with all but the largest of dendrimers. For very high generations, the surface of the dendrimer could become quite crowded and possibly prevent other molecules from entering the dendrimer and reaching the catalytic site.[5d,11]

Results and Discussion

In our study, two different techniques were applied to measure electron transfer within this family of porphyrin-core dendrimers. The first technique was cyclic voltammetry, which provides information on intensity and rate of electron transfer between a redox-active molecule and an electrode surface. These data may, in turn, be correlated to both the electrochemical environment and the steric hindrance resulting from the presence of the dendrimers. To transfer an electron, the porphyrin moiety must come to within 10 Å of the electrode surface. If the dendrimer surrounding the porphyrin core restricts its access to the electrode surface, electron transfer will be inhibited. This inhibition will be apparent in the cyclic voltammogram as a decrease in the peak current, an increase in the potential difference, and a broadening of the voltammetric wave. Additionally, cyclic voltammetry can provide

(5) (a) Dandliker, P. J.; Diederich, F.; Gross, M.; Knobler, C. B.; Louati, A.; Sanford, E. M. *Angew. Chem., Int. Ed. Engl.* **1994**, *33*, 1739. (b) Jin, R.; Aida, T.; Inoue, S. *J. Chem. Soc., Chem. Commun.* **1993**, 1260. (c) Pollak, K. W.; Leon, J. W.; Fréchet, J. M. J. *Polym. Mater. Sci. Eng.* **1995**, *73*, 137−138. (d) Tomoyose, Y.; Jiang, D.; Jin, R.; Aida, T.; Yamashita, T.; Horie, K.; Yashima, E.; Okamoto, Y. *Macromolecules* **1996**, *29*, 5236. (e) Jiang, D; Jin, R. Aida, T. *J. Chem. Soc., Chem. Commun.* **1996**, 1523. (f) Bhyrappa, P.; Young, J. K.; Moore, J. S.; Suslick, K. S. *J. Am. Chem. Soc.* **1996**, *118*, 5708. (g) Collman, J. P.; Fu, L.; Zingg, A.; Diederich, F. *J. Chem. Soc., Chem. Commun.* **1997**, 193. (h) Sadamoto, R.; Tomioka, N.; Aida, T. *J. Am. Chem. Soc.* **1996**, *118*, 3978−9.

(6) (a) Hawker, C. J.; Fréchet, J. M. J. *J. Am. Chem. Soc.* **1990**, *112*, 7638. (b) Fréchet, J. M. J. *Science* **1994**, *263*, 1710.

(7) (a) Tomalia, D. A.; Naylor, A. M.; Goddard, W. A. *Angew. Chem., Int. Ed. Engl.* **1990**, *29*, 138.

(8) (a) Mourey, T. H.; Turner, S. R.; Rubinstein, M.; Fréchet, J. M. J.; Hawker, C. J.; Wooley, K. L. *Macromolecules* **1992**, *25*, 2401. (b) Hawker, C. J.; Wooley, K. L.; Fréchet, J. M. J. *J. Am. Chem. Soc.* **1993**, *115*, 4375. (c) Saville, P. M.; White, J. W.; Hawker, C. J. Wooley, K. L.; Fréchet, J. M. J. *J. Phys. Chem.* **1993**, 97, 293. (d) Saville, P. M.; Reynolds, P. A.; White, J. W.; Hawker, C. J.; Wooley, K. L.; Fréchet, J. M. J. *J. Phys. Chem.* **1995**, *99*, 8283. (e) Saville, P. M.; Reynolds, P. A.; White, J. W.; Hawker, C. J.; Fréchet, J. M. J.; Wooley, K. L.; Penfold, J.; Webster, J. R. P. *J. Phys. Chem.* **1995**, *99*, 8283.

(9) Hawker, C. J.; Wooley, K. L.; Fréchet, J. M. J. *J. Chem. Soc., Chem. Commun.* **1994**, 925.

(10) (a) Kim, Y. H.; Webster, O. W. *J. Am. Chem. Soc.* **1990**, *112*, 4592. (b) Newkome, G. R.; Moorefield, C. N.; Baker, G. R.; Saunders, M. J.; Grossman, S. H. *Angew. Chem., Int. Ed. Engl.* **1991**, *30*, 1178. (c) Hawker, C. J.; Wooley, K. L.; Fréchet, J. M. J. *J. Chem. Soc., Perkin Trans. 1* **1993**, 1287.

(11) (a) Jansen, J. F. G. A.; de Brabander-van den Berg, E. M. M.; Meijer, E. W. *Science* **1994**, *266*, 1226. (b) Jansen, J. F. G. A.; Meijer, E. W. *J. Am. Chem. Soc.* **1995**, *117*, 4417.

(12) (a) Kawa, M.; Fréchet, J. M. J. *Chem. Mater.*, in press. (b) Gorman, C. B.; Parkhurst, B. L.; Su, W. L.; Chen, K. Y. *J. Am. Chem. Soc.* **1997**, *119*, 1141.

(13) Gitsov, I.; Ivanova, P. T.; Fréchet, J. M. J. *Macromol. Rapid Commun.* **1994**, *15*, 387.

(14) Hawker, C. J.; Wooley, K. L.; Fréchet, J. M. J. *J. Am. Chem. Soc.* **1993**, *115*, 4375.

(15) (a) Guillet, J. *Polymer Photophysics and Photochemistry*; Cambridge University Press: New York, 1985. (b) Winnik, M. A. *Photophysical and Photochemical Tools in Polymer Science*; Kluwer Academic Press: Boston, 1985.

(16) (a) Moreno-Bondi, M. C.; Orellana, G.; Turro, N. J.; Tomalia, D. A. *Macromolecules* **1990**, *23*, 910. (b) Turro, N. J.; Barton, J. K.; Tomalia, D. A. *Acc. Chem. Res.* **1991**, *24*, 332.

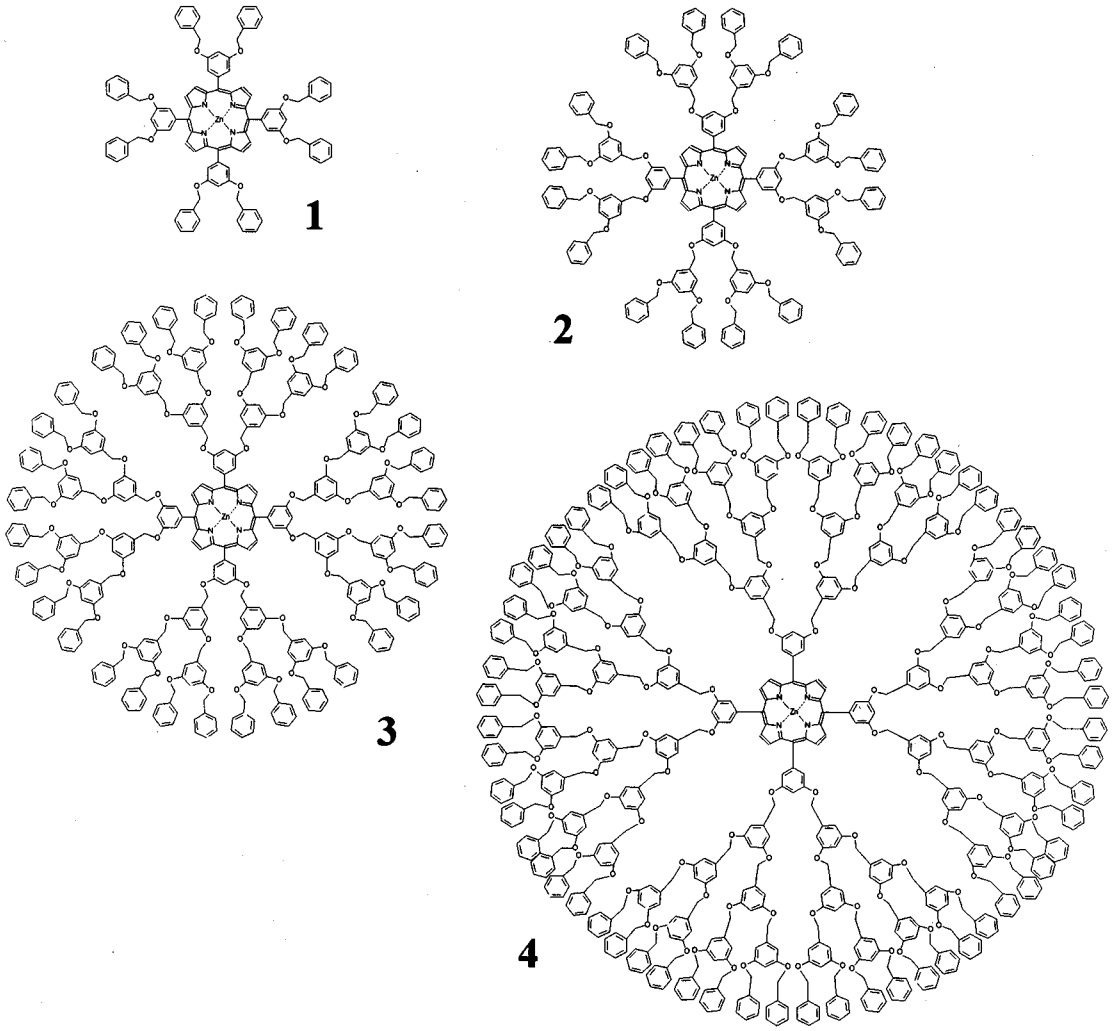

Figure 1. Series of porphyrin-core dendrimers prepared and studied in this report: **1**, Zn[G−1]$_4$P; **2**, Zn[G−2]$_4$P; **3**, Zn[G−3]$_4$P; **4**, Zn[G−4]$_4$P.

information on the electrochemical interaction between the porphyrin moiety and the dendrimer itself.[17] If the presence of the dendrimer causes a shift in the formal potential, then electrochemical interaction between the porphyrin core and the dendritic substituents can be inferred. From knowledge of such interactions, one could then ascertain whether these metalloporphyrin-core dendrimers could be designed to operate as catalysts without fear of the dendrimer interfering with the behavior of the catalytic site.

The second technique used to measure electron transfer was fluorescence quenching by a small molecule, benzylviologen. To accept the photoexcited electron, the quencher must come to within 4 Å of the porphyrin moiety. As in the previous experiment, the dendrimer surrounding the porphyrin might well inhibit access to its active site, thereby reducing the quenching efficiency. The efficiency of benzylviologen to quench the fluorescence of photoexcited metalloporphyrin-core dendrimers was measured through Stern−Volmer analyses. Additionally, the UV/vis absorption and emission spectra of pure solutions of each metalloporphyrin-core dendrimer were measured and analyzed to determine the effect of the dendrimer on the metalloporphyrin's photophysical behavior.

If specially designed porphyrin-core dendrimers are to be used as catalysts for transformations involving small molecules, then the dendrimer should not block access to the catalytic site; therefore, it was hoped that no significant decrease in quenching efficiency would be seen as the dendrimer generation was increased.

Synthesis of Porphyrin-Cored Dendrimer. The first-generation porphyrin-core dendrimer (Figure 1) was prepared through a Lindsey type synthesis[18] involving acid-catalyzed condensation of 3,5-dibenzyloxybenzaldehyde with pyrrole, followed by an oxidation step. After isolating the free-base product, the porphyrin core was metalated with zinc. The overall yield was 40%.

The second through fourth generation porphyrin-core dendrimers, also shown in Figure 1, were prepared by alkylating zinc tetrakis(3,5-dihydroxyphenyl)porphyrin with the appropriate bromide dendron in a Williamson ether synthesis (Scheme 1). The reaction is best per-

(17) (a) Dolphin, D. *The Porphyrins*; Academic Press: New York, 1978; Vol. V, 30−35. (b) Falk, J. E. *Porphyrins and Metalloporphyrins*; Elsevier: New York, 1964; pp 69−71.

(18) Lindsey, J.; Scheirman, I.; Hsu, H.; Kearney, P.; Marguerettaz, A. *J. Org. Chem.* **1987**, *52*, 827.

Scheme 1

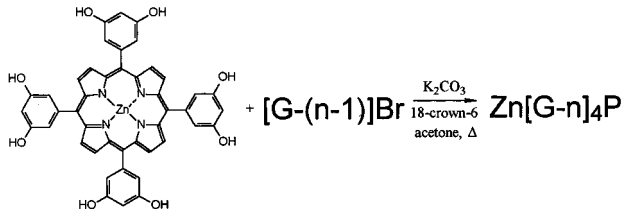

Compound Number	Generation	Nomenclature
1	n = 1	Zn[G-1]$_4$P
2	n = 2	Zn[G-2]$_4$P
3	n = 3	Zn[G-3]$_4$P
4	n = 4	Zn[G-4]$_4$P

formed under nitrogen atmosphere, using potassium carbonate and 18-crown-6 in dry acetone at 60 °C. Temperatures higher than 60 °C produced significant C-alkylation of the phenyl ring bound to the porphyrin core, evident in analysis of the product by ^{1}H NMR as two resonances of equal intensities at 7.82 and 8.59 ppm generated by the two remaining phenyl protons of the C-alkylated moiety. The O-alkylation reaction was monitored by TLC and continued until no starting porphyrin was seen on the baseline. Yields for the second-, third-, and fourth-generation porphyrin-cored dendrimer were 71%, 68%, and 20%, respectively. Proton NMR showed the products to be fully alkylated at the phenolic oxygen. Similarly, MALDI-TOF mass spectroscopy showed a single product at the expected molecular weight ($M + Na^+$ and $M + K^+$), and UV/vis spectrometry confirmed that the porphyrin core was intact.

Cyclic Voltammetry. Voltammograms were recorded for solutions of the porphyrin-core dendrimers with 0.1 M tetrabutylammonium perchlorate (TBAP). Whereas oxidative processes were measured for solutions of porphyrin-cored dendrimers in dichloromethane (CH_2Cl_2), reductive processes were measured in dimethylformamide (DMF). The peak current is proportional to the number of electrons transferred between the porphyrin core and the electrode, and the peak potential difference, ΔE_p, reflects the kinetics of electron transfer. If enough dendrimer surrounds the porphyrin to restrict its access to the electrode surface, then the electron transfer will become inhibited affecting both the peak currents and ΔE_p values. Moreover, shifts in the values of the formal potential provide an indication of the nature and magnitude of the interaction between the dendrimer and the core. If the formal potentials remain unchanged throughout the series of porphyrin-cored dendrimers, then one could surmise that the dendrimer does not directly interfere with the porphyrin's electrochemical activity. The cyclic voltammograms depicting oxidative and reductive processes are shown in Figures 2 and 3, respectively. Wave potentials and potential differences are tabulated in Table 1.

(a) Oxidative Cycle. In CH_2Cl_2, dendrimer **1** exhibits two reversible one-electron events at +0.81 V and +1.08 V, forming the mono- and dication, respectively (Figure 2). These values, as well as their separation of 170 mV, match well with the values typically observed for oxidations involving small metalloporphyrins in non-

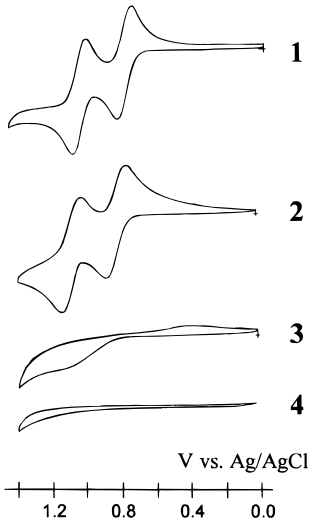

Figure 2. Anodic cyclic voltammograms for porphyrin-core dendrimers **1**, **2**, **3**, and **4**. Current in mA.

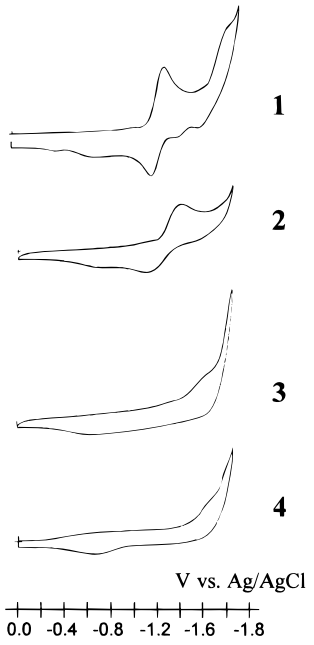

Figure 3. Cathodic cyclic voltammograms for porphyrin-core dendrimers **1**, **2**, **3**, and **4**. Current in mA.

Table 1. Redox Potentials for the Porphyrin-Core Dendrimers[a]

dendrimer	$E°_{ox}$ (I)[b]	$E°_{ox}$ (II)[b]	$E°_{red}$ (I)[c]	$E°_{red}$ (II)[c]
ZnTPP	0.83 (70)	1.12 (80)	−1.21 (75)	−1.62 (110)
1	0.81 (90)	1.08 (70)	−1.22 (110)	−1.68 (240)
2	0.82 (125)	1.08 (105)	−1.37 (240)	
3	1.12[d]		−1.55[d]	
4			−1.61[d]	

[a] Values for zinc-tetraphenylporphyrin are included for comparison of our porphyrin-core dendrimers to conventional metalloporphyrins. V vs Ag/AgCl (ΔE_p in mV); scan rate 0.1 V/s. [b] In CH_2Cl_2 (0.1 M TBAP). [c] In DMF (0.1 M TBAP). [d] Shoulder.

nucleophilic solvents.[19] In DMF, the first oxidation (+0.98 V) is still reversible, but the second oxidation (+1.23 V), forming the dication, becomes chemically and electrochemically irreversible. This phenomenon is also

(19) (a) Kadish, K. M. In *Progress in Inorganic Chemistry*; Wiley: New York, 1986; Vol. 34, pp 566−571. (b) Dolphin, D. *The Porphyrins*; Academic Press: New York, 1978; Vol. V, pp 55−70.

common for small metalloporphyrins.[19] The first anodic cycle of dendrimer **2** in CH_2Cl_2 exhibits two electrochemically quasi-reversible oxidations with formal potentials of +0.81 and +1.08 V. The trend toward electrochemical and chemical irreversibility is also observed as the generation number increases from one to two and accelerates when going to higher generations. Dendrimer **3** shows just one ill-defined and irreversible oxidation, and dendrimer **4** exhibits no oxidative process.

A dramatic change is observed in the cyclic voltammograms of the higher generations of these porphyrin-core dendrimers. As the dendrimer generation increases, the intensities of the oxidative processes decrease. The most dramatic change is observed when comparing generations two and three. In the latter case, a drastic decrease in the peak current and a significant increase in the ΔE_p value are observed. Both of these changes are consistent with a strong steric inhibition to electron transfer for the third generation dendrimer. For generation four, the steric inhibition effect is so pronounced that no oxidative process can be seen at all. These data demonstrate the effectiveness of isolating a reactive site from a surface by surrounding it with a dendrimer shell. It should be noted that as the dendrimer generation increases, the observed formal potentials do not shift significantly, suggesting that the dendrimer shell itself does not interact strongly with the porphyrin moiety.

(b) Reductive Cycle. At negative potentials, two reductions of dendrimer **1** at −1.22 and −1.68 V are observed in DMF, forming the mono- and dianion, respectively (Figure 3). Whereas the first is completely reversible, the second leads partially to the formation of phlorin ([**1**H]$^{\bullet}$) by reaction with the solvent.[19a] The electrochemical irreversibility of the second wave is even more apparent in CH_2Cl_2. Evidence for the steric effect of the bulky dendritic substituents on the cathodic processes is seen more readily than is the case for the corresponding anodic cycles. The voltammogram of dendrimer **2** shows just one quasi-reversible wave with a formal potential of −1.37 V, while dendrimer **3** exhibits only a small, completely irreversible shoulder at −1.55 V. Dendrimer **4** exhibits the same blurred features with a slight shift of the cathodic wave to −1.61 V.

As the dendrimer generation increases, the intensities of the reductive process decrease. Unlike the oxidative processes where a dramatic decrease is seen through the series, the reductive processes exhibit a more gradual decrease in peak intensity as the dendrimer generation increases from one to four. Nevertheless, these data also demonstrate the effectiveness of the dendrimer in isolating the porphyrin site from the electrode surface. As was the case for the anodic scans, the observed formal potentials for the cathodic processes do not shift significantly, suggesting, again, that the dendrimer does not interact with the porphyrin moiety.

These observations are quite different from those reported by Diederich and co-workers[5a] for a structurally distinct family of porphyrin-cored dendrimers. Their molecules displayed irreversibility in both the cathodic and anodic cycles only for the third-generation dendrimer, whereas our porphyrin-core dendrimers already exhibit a decrease in electroactivity in the cathodic cycle for the second-generation dendrimer. Anodic cycles for our dendrimers show irreversibility at the third generation. This is likely related to the ability of the relatively rigid benzyl ether dendrimer to hinder the approach of the porphyrin core to the electrode. In addition, the presence of the benzyl ether dendrimer shell has no significant effect on the values of the formal potentials in contrast to the results of Diederich et al.[5a] As shown in the computer-generated model of our fourth-generation dendritic porphyrin (Figure 4), the 3,5-substitution pattern of the porphyrin-bound phenyl group directs the dendrons away from the porphyrin core, thereby minimizing interactions between the dendrimer and the porphyrin. In contrast, Diederich's very interesting porphyrin-core dendrimers have a 2,6-substitution pattern that provides a more close-packed environment in which the dendrons are placed directly over the faces of the porphyrin, thereby facilitating interactions and leading to a shift in the redox potentials as the dendrimer generation is increased. We have recently shown that the substitution pattern of dendrons (e.g., 1,2,5- vs 1,3,5-substituted aromatic ring connecting to the core moiety) can significantly affect the properties of the core.[11a] Our results suggest that our porphyrin-core dendrimers are readily amenable to current porphyrin-catalyzed chemistries, and in light of Diederich's interesting findings,[5a] rate enhancing ligands or substrate binding sites, if desired, could be incorporated in the dendrimer architecture and directed toward the catalyst's active site. Because of the high degree of structural control afforded by the convergent approach,[6] the placement of such reactive moieties might be conveniently achieved through the convergent synthesis route.[12a]

Photophysical Studies. All measurements were made on solutions of the metalloporphyrin-core dendrimer in solutions of dimethylformamide (DMF). The solutions were degassed by purging with DMF-saturated argon. In the absorption and emission spectra, peak values are affected by interactions between the chromophore and ligands, solvent, etc. Therefore, when comparing the spectra for the series of metalloporphyrin-core dendrimers, the wavelengths absorbed or emitted will shift if the dendritic substituents ligate the zinc cation or exert $\pi-\pi$ interactions with the porphyrin. In the fluorescence-quenching experiments, access of a small molecule to the porphyrin core is assessed through Stern−Volmer analyses. As the generation of the dendrons surrounding the metalloporphyrin core increases, steric congestion about the core increases, and this, in turn, may affect the ability of electron-acceptor moieties to reach the core.

(a) Absorption and Emission Spectra. The absorption (Figure 5) and emission spectra of the porphyrin-core dendrimers are typical of metalloporphyrins.[20,21] For example, zinc tetraphenylporphyrin exhibits a Soret absorption at 424 nm and Q-bands at 559 and 599 nm. All of the zinc porphyrin-cored dendrimer exhibit Soret bands at 430 nm and Q-band absorptions at 560 and 600 nm. When excited at 420 nm, zinc tetraphenylporphyrin emits at 605 nm (singlet decay) and 659 nm

(20) (a) Dolphin, D. *The Porphyrins*; Academic Press: New York, 1978; Vol. III, pp 12−16. (b) Falk, J. E. *Porphyrins and Metalloporphyrins*; Elsevier: New York, 1964; pp 75−76, 243−246.

(21) Falk, J. E. *Porphyrins and Metalloporphyrins*; Elsevier: New York, 1964; pp 85−87.

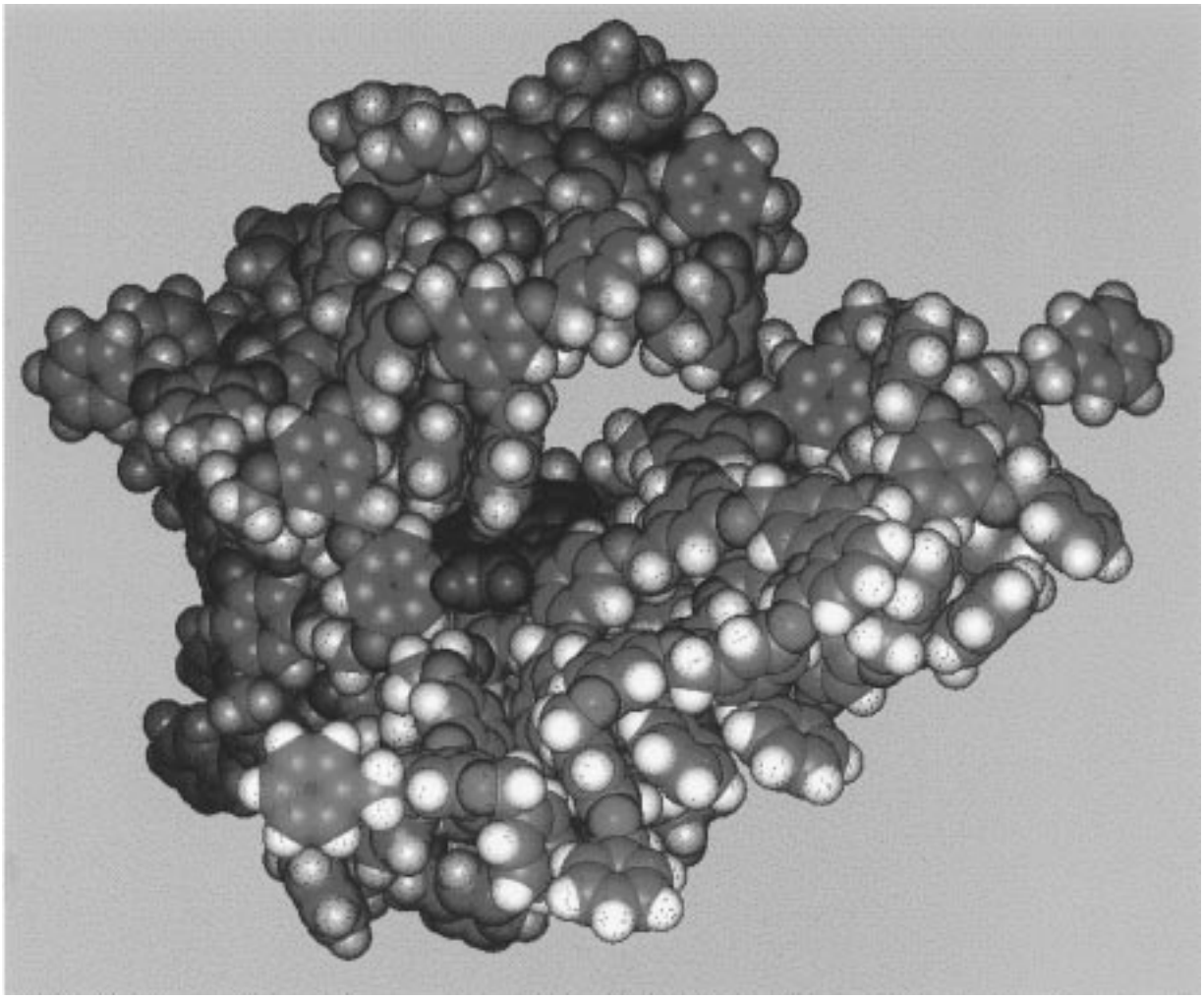

Figure 4. Space-filling model of the fourth-generation dendritic porphyrin **4**. The core is highlighted in purple.

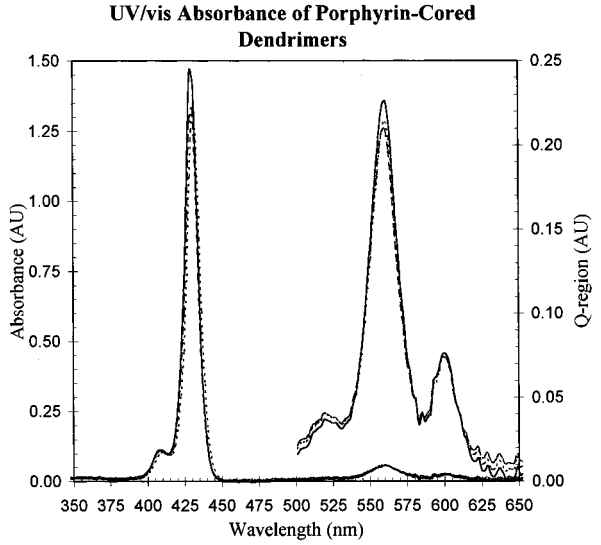

Figure 5. UV/vis absorbance spectra for **1** (—), **2** (– – –), and **4** (· · ·). Q-region is expanded for clarity.

(triplet decay). When excited at 425 nm, all four of the porphyrin-core dendrimers also emit at 605 nm (singlet decay) and at 659 nm (triplet decay).

The difference in wavelength absorptions of the porphyrin-core dendrimers compared to tetraphenylporphyrin are due to the alkoxy substituents present on the porphyrin-bound phenyl rings.[20] As the dendrimer generation increases, absorption and fluorescence bands do not shift, suggesting again that the dendrons which are directed away from the porphyrin core do not interact with the chromophore.[21] As a result, the dendritic substituents are not expected to alter either the nature of the photoexcitation or the subsequent photophysical processes of the porphyrin moiety.

(b) Fluorescence Quenching Experiments. The metalloporphyrin was excited by irradiating the solution at a wavelength of 425 nm, and the intensity of the emission at 605 nm was measured and plotted as a function of viologen concentration. From this plot, the $k_q t$ values (the product of the quenching rate constant by excited-state lifetimes) were calculated and compared for the series of porphyrin-cored dendrimers (Figure 6). Assuming that excited-state lifetimes are constant throughout the series, quenching appears to be somewhat hindered (9% less efficient) when the dendrimer size is increased from dendrimer **1** to dendrimer **2**. For the third-generation dendrimer **3**, quenching remains the same but it becomes 33% more efficient for the fourth-generation dendrimer **4**. This apparent enhancement of the quenching efficiency observed for dendrimer **4** could be the result of the large dendritic substituents affecting either the rate of quenching or the excited-state lifetime of the porphyrin core. Because these two values have not been deconvoluted from the Stern–Volmer measurement, an exact explanation for this

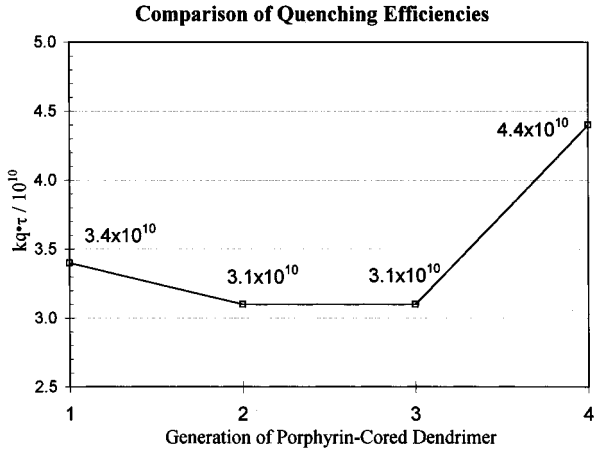

Figure 6. Results of Stern−Volmer analysis of **1**, **2**, **3**, and **4**. Data points are labeled with $k_q t$ values.

modest enhancement is not available. Inoue and co-workers[5b] have prepared convergent benzyl ether dendrimers with porphyrin cores and compared the rate of quenching of a fourth-generation dendrimer with that of a first generation dendrimer. When 2-methyl-1,4-naphthoquinone (vitamin K_3) is used as the small molecule electron acceptor, a higher rate of quenching was observed for the larger dendrimer.[5b] This observation correlates well with our data.

To quench the fluorescence of the porphyrin, the molecular orbitals of the photoexcited porphyrin and the quencher must experience a significant overlap.[15a] To achieve this, the electron acceptor must come within 4 Å of the face of the porphyrin moiety. Our findings may be rationalized by considering that the increase in quenching efficiency of **4** is likely the result of both $\pi-\pi$ attractions and the globular conformation of the dendrimer. The electron poor π-system of the electron acceptor is attracted to the electron-rich π-systems of the dendrons. Because the dendrons are in close proximity to the porphyrin (Figure 4), the acceptor is readily available to quench the porphyrin fluorescence. Aida and co-workers have recently reported long-range electron transfer in a somewhat similar water-soluble electron donor/acceptor system.[5h] In their system, the positively charged quencher is believed to be attracted to the negatively charged surface of the water-soluble dendrimer. Long-range electron transfer in analogous small-molecule charge-transfer assemblies is known;[15a] however, it is not the expected mechanism of fluorescence quenching of our uncharged porphyrin-core dendrimers. It is also becoming apparent that, in some cases, the poly(aryl ether) dendrons permit long-range energy transfer via an antenna effect.[12a] However this phenomenon probably does not occur in this particular system because the fluorescence spectrum of the porphyrin core and the absorption spectrum of the viologen (λ_{max} = 310 nm) lack the necessary spectral overlap. Regardless of the exact mechanism of fluorescence quenching, these experiments confirm that although the porphyrin is surrounded by large dendrons, the shell of the fourth-generation macromolecule is not so crowded that it would prevent a small guest molecule from entering. This finding, which confirms earlier results[10,11] demonstrating the use of a dendrimer as a host to small molecules, is important since our target is to use dendritic porphyrins in the catalytic transformation of small molecules.

Conclusion

These electron-transfer experiments demonstrate the ability of the dendrimer to isolate their porphyrin core from an electrode by sterically limiting access of the core to the electrode surface. Surrounding the metalloporphyrin core with higher generation dendrons increases the distance between the porphyrin core and the electrode surface, thereby decreasing the opportunity to achieve electron transfer. However, while high-generation dendrimers can isolate a site from a surface, they do not generally restrict access by a small molecule. This is especially true if the small molecule is attracted to the dendrimer. As a result of their ability to be penetrated by small molecules, benzyl phenyl ether dendrimers with metalloporphyrin cores could potentially be employed as catalysts. Metalation of their cores is possible using conventional approaches, while the modification of their periphery allows their fine-tuning for specific applications. Because the dendritic shell does not interfere with the photoexcitation or subsequent photochemical processes of the porphyrin core, these porphyrin-core dendrimers may be useful in conventional porphyrin-catalyzed chemistries. Specially designed dendrons with precise architectures incorporating rate enhancing ligands, guest-binding clefts, or solubilizing moieties, could be prepared using the convergent route to afford better performing porphyrin-core dendrimers.

Experimental Section

Cyclic Voltammetry. Tetra-*n*-butylammonium perchlorate (TBAP, GFS Chemicals) was recrystallized three times from ethyl acetate and dried under vacuum at 90 °C for 72 h. Dichloromethane (CH_2Cl_2) and *N*,*N*-dimethylformamide (DMF, Burdick & Jackson, distilled in glass) were dried over 4 Å molecular sieves. Cyclic voltammograms were obtained using an IBM EC-225 voltammetric analyzer. Data were recorded on a Soltec VP-64236 *X*−*Y* recorder. Three compartment cells of conventional design were employed and potentials were measured against a sodium chloride silver/silver chloride (Ag/AgCl) electrode without regard for the liquid junction potential. A coiled platinum wire served as the counter electrode, and a polycrystalline platinum electrode sealed in glass was employed as the working electrode. Measurements were carried out in 0.1 M TBAP solutions containing 1 mM of substrate.

Fluorescence Studies. Absorption spectra were measured as solutions in dimethylformamide (DMF) (Aldrich, stored over molecular sieves, 4 Å) on a Hewlett-Packard 8452A diode array spectrophotometer in glass cells (10 mm path length). Fluorescence spectra were also measured in DMF (as described above plus degassed by bubbling DMF-saturated argon) on a SLM Instruments AMINCO spectrofluorometer equipped with a xenon lamp.

General Directions. Silica for flash chromatography was Merck silica gel 60 (230−400 mesh). Matrix-assisted laser-desorption ionization time-of-flight (MALDI-TOF) mass spectroscopy was performed on a Finnigan Lasermat. The energy source was a 337 nm nitrogen laser. Samples were prepared as 10 mg/mL solutions in tetrahydrofuran (THF). The matrix was a 0.3 M solution of indole acrylic acid in THF. 5 mL of the sample and 10 mL of matrix were combined and analyzed. All NMR spectra were recorded as solutions in $CDCl_3$ on a Bruker WM 300 (300 MHz) spectrometer with the solvent proton signal as standard: 7.24 for ^1H and 77.0 for ^{13}C. The following abbreviations are used: Dendritic zinc-metalated

porphyrins are referred to as Zn[G−*n*]$_4$P, where n designates the dendrimer generation. Ar refers to the aromatic repeat units within the dendrimer. Ph refers to the phenyl chain ends or "surface" groups of the dendrimer. Bn refers to the benzylic positions of the dendrimer. Porph refers to the porphyrin ring, a and b refer to the corresponding sites on the pyrrole rings of the porphyrin, and pyr refers to the pyridyl rings of benzylviologen.

General Procedure for the Preparation of the Benzylic Alcohol Dendrons.[6] A mixture of the appropriate benzylic bromide dendron (2.05 equiv), 3,5-dihydroxybenzyl alcohol (1.00 equiv), dried potassium carbonate (2.50 equiv), and 18-crown-6 (0.20 equiv) in dry acetone was heated at reflux and stirred vigorously under nitrogen for 48 h. The mixture was allowed to cool and evaporated to dryness under reduced pressure. The residue was partitioned between water and CH_2Cl_2 and the aqueous layer extracted with CH_2Cl_2. The combined organic extracts were dried ($MgSO_4$) and evaporated to dryness. The crude product was purified by column chromatography. Analyses agreed with those published.[6a]

General Procedure for the Preparation of the Benzylic Bromide Dendrons.[6a] To a mixture of the appropriate benzylic alcohol dendrons (1.00 equiv) and carbon tetrabromide (1.25 equiv) in a minimum amount of dry THF was added triphenylphosphine (1.25 equiv), and the reaction mixture was stirred under nitrogen for 20 min. The reaction mixture was then poured onto water and extracted with CH_2Cl_2. The combined organic extracts were dried ($MgSO_4$) and evaporated to dryness. The crude product was purified by column chromatography. Analyses agreed with those published.[6a]

Tetrakis(3,5-dimethoxyphenyl)porphyrin. 3,5-Dimethoxybenzaldehyde (1.500 g, 9.026 mmol) and freshly distilled pyrrole (626 mL, 9.026 mmol) were dissolved in dry chloroform (903 mL) under nitrogen atmosphere. After adding $BF_3{\cdot}OEt_2$ (364 μL, 2.979 mmol) to the mixture, the solution was shielded from ambient light and stirred at room temperature for 90 min. After adding DDQ (1.537 g, 6.770 mmol), the mixture was stirred for an additional 90 min, then triethylamine (415 μL, 2.979 mmol) was added to neutralize the acid. The solvent was evaporated, and the residual solids were adsorbed onto silica (20 mL). The crude product was purified by chromatography through a 40 mL silica column eluting with a linear gradient starting with pure hexane and ending with pure CH_2Cl_2. After collecting the product fractions and evaporating the solvent, the product was obtained as purple crystals, yield 52% UV/vis abs (ϵ) 424 nm (280 000), 516 nm (19 000), 548 nm (9000), 586 nm (9000), 648 nm (5000). ^{1}H NMR (in DMSO-d_6, 2.49 ppm) δ 8.95 (s, 8 H, β-*H*); 7.01 (s, 8 H, Ar−*H*); 6.65 (s, 4 H, Ar−*H*); 3.33 (s, 24 H, ArO−C*H*$_3$); −3.07 (s, 2 H, N−*H*). ^{13}C NMR (in DMSO-d_6, 39.5 ppm) δ 156.60 (Ar*C*−OCH$_3$); 142.89 (Ar*C*−porph); 131.12 (β *C*); 119.94 (meso *C*); 114.19, 102.28 (Ar*C*−H); 48.64 (Ar−O*C*H$_3$). Anal. Calcd for $C_{52}H_{46}N_4O_8$: C 73.05, H 5.42, N 6.55. Found: C 73.11, H 5.29, N 6.43.

Tetrakis(3,5-dihydroxyphenyl)porphyrin. Tetra(3,5-dimethoxyphenyl)porphyrin (740 mg, 0.866 mmol) was dissolved in dry CH_2Cl_2 (20 mL) under nitrogen atmosphere. The solution was cooled to 0 °C, and then BBr_3 (7.27 mL, 7.271 mmol, 1 M in CH_2Cl_2) was slowly added to the reaction. After addition, the mixture was allowed to warm to room temperature as it stirred overnight. Enough methanol was then added to deactivate any unreacted BBr_3. Then distilled water (30 mL) was added, and the mixture was stirred for 2 h. After evaporation of the organic solvents, a green powder was filtered from the water. It was dissolved in ether, washed twice with saturated $NaHCO_3$, washed once with distilled water, and then dried over Na_2SO_4. The solvent was evaporated, and the product was isolated as purple crystals that were dried under vacuum at 40 °C (yield 100%). UV/vis abs (ϵ) 424 nm (242 000), 516 nm (14 000), 552 nm (5000), 592 nm (4000), 648 nm (2000). ^{1}H NMR (in DMSO-d_6, 2.49 ppm) δ 8.93 (s, 8 H, β-*H*); 7.05 (s, 8 H, Ar−*H*); 6.64 (s, 4 H, Ar−*H*); 3.81 (s, broad, Ar−O*H*). ^{13}C NMR (in DMSO-d_6, 39.5 ppm) δ 156.54 (Ar*C*−OH); 144.97 (Ar*C*−porph); 127.50 (β *C*); 117.81 (meso *C*); 114.15, 102.50 (Ar*C*−H). Mass spectrum (MALDI-TOF) *m*/*z* calculated 742.7; found 752.7.

Zinc Tetrakis(3,5-dihydroxyphenyl)porphyrin. Tetrakis(3,5-dihydroxyphenyl)porphyrin (700 mg, 0.942 mmol) and $Zn(OAc)_2{\cdot}2H_2O$ (228 mg, 1.043 mmol) were dissolved in methanol (20 mL). The solution was heated to reflux for 4 h, then distilled water (60 mL) was added, and the methanol was evaporated under vacuum. The turbid solution was placed in the refrigerator overnight, and the purple crystalline product was filtered and dried in vacuo at 40 °C (yield 99%). UV/vis abs (ϵ) 428 nm (523 000), 560 nm (20 000), 600 nm (7000). ^{1}H NMR (in DMSO-d_6, 2.49 ppm) δ 9.60 (s, 8 H, Ar−O*H*); 8.86 (s, 8 H, β-*H*); 7.01 (d, 8 H, Ar−*H*); 6.62 (t, 4 H, Ar−*H*). ^{13}C NMR (in DMSO-d_6, 39.5 ppm) δ 156.21 (Ar*C*−OH); 148.93 (α *C*); 144.46 (Ar*C*−porph); 131.33 (β *C*); 120.23 (meso *C*); 114.16, 101.72 (Ar*C*−H). Mass spectrum (MALDI-TOF) *m*/*z* calculated 806.1; found 813.9.

Zn[G−1]$_4$P. A mixture of 3,5-dibenzyloxybenzaldehyde (1.500 g, 4.711 mmol) and freshly distilled pyrrole (327 mL, 4.711 mmol) were dissolved in dry chloroform (903 mL) under nitrogen. Then $BF_3{\cdot}OEt_2$ (190 mL, 1.555 mmol) was added to the reaction, and the mixture was shielded from ambient light as it stirred at room temperature for 90 min. After adding DDQ (802 mg, 3.534 mmol), the reaction mixture was stirred for an additional 90 min, and then triethylamine (217 mL, 0.157 mmol) was added to neutralize the acid. The solvent was evaporated, and the residual solids were separated by column chromatography through a 40 mL silica column eluting with a linear gradient starting with pure hexane and ending with pure CH_2Cl_2. After collecting the product fractions and evaporating the solvent, the product was collected as purple crystals (41%). Tetrakis(3,5-dibenzyloxyphenyl)porphyrin (500 mg, 0.342 mmol) and $Zn(OAc)_2{\cdot}2H_2O$ (82 mg, 0.376 mmol) were dissolved in chloroform/methanol (1:1, 100 mL). The solution was heated at reflux for 5 h, then was cooled to room temperature, and the solvent evaporated. Residual solids were partitioned between water and ether. The ether layer was separated, and solvent was evaporated to afford purple crystals (99%). UV/vis abs (ϵ) 428 nm (568 000), 560 nm (22 000), 600 nm (7000). ^{1}H NMR δ 8.98 (s, 8 H, β-*H*); 7.48 (d, 8 H, Ar−*H*); 7.35 (m, 40 H, Ph−*H*); 7.02 (t, 4 H, Ar−*H*); 5.18 (s, 16 H, Bn−*H*). ^{13}C NMR δ 157.78 (Ar *C*−O); 149.89 (α *C*); 144.63 (Ar *C*−porph); 136.75 (Ph *C*−CH$_2$); 131.97 (β *C*); 128.58, 128.01, 127.63 (Ph *C*−H); 120.67 (meso *C*); 115.06, 96.67 (Ar *C*−H). Mass spectrum (MALDI-TOF) *m*/*z* calculated 1527.1; found 1538.1. Anal. Calcd for $C_{100}H_{76}N_4O_8Zn$; C 78.65, H 5.02, N 3.67. Found: C 78.60, H 5.05, N 3.54.

Preparation of Porphyrin-Core Dendrimers (Generations 2−4). The second-, third-, and fourth-generation porphyrin-core dendrimers were synthesized by coupling zinc tetrakis(3,5-dihydroxyphenyl)porphyrin to the appropriate benzylic bromide dendron in a Williamson ether synthesis. Zinc tetrakis(3,5-dihydroxyphenyl)porphyrin (1.00 equiv) and the dendritic bromide (9.60 equiv) were dissolved in acetone under nitrogen atmosphere. To this solution, K_2CO_3 (16.0 equiv) and 18-crown-6 (1.60 equiv) were added, and the mixture was stirred and warmed to 60 °C. The solvent was evaporated, and the residual solids were partitioned between water and CH_2Cl_2. The layers were separated, and the aqueous layer was extracted with CH_2Cl_2 (3×). The solvent was evaporated, and the residual solids were adsorbed onto silica (20 mL), and the crude product was purified by chromatography through a 40 mL silica column eluting with a linear gradient starting with pure hexane and ending with pure CH_2Cl_2. The product fractions were collected, and the solvent was evaporated. The product was dissolved in a minimum amount of $CHCl_3$ then precipitated into methanol. The precipitate was then dissolved in a minimum amount of ethyl acetate and reprecipitated into ethyl ether. The product was obtained as a dark purple powder.

Zn[G−2]$_4$ P. This was prepared as above from zinc tetrakis(3,5-dihydroxyphenyl)porphine and [G−1]Br, yield 71% UV/vis abs (ϵ) 428 nm (498 000), 560 nm (20 000), 600 nm (7000). ^{1}H NMR δ 9.18 (s, 8 H, β-*H*); 7.48 (d, 8 H, Ar−*H*); 7.33 (m, 80 H, Ph−*H*); 7.03 (t, 4 H, Ar−*H*); 6.73 (d, 16 H, Ar−

H); 6.56 (t, 8 H, Ar−*H*); 5.06 (s, 16 H, Bn−*H*); 4.96 (s, 32 H, Bn−*H*). ^{13}C NMR δ 160.09, 157.71 (Ar *C*−O); 149.92 (α *C*); 144.80 (Ar *C*−porph); 139.15 (Ar *C*−CH_2); 136.63 (Ph *C*−CH_2); 132.10 (β *C*); 128.46, 127.88, 127.43 (Ph *C*−H); 120.67 (meso *C*); 115.02, 106.43, 101.65, 96.66 (Ar *C*−H); 70.00 (Ar/Ph−*C*H_2). Mass spectrum (MALDI-TOF) *m*/*z* calculated 3225.1; found 3228.3. Anal. Calcd for $C_{212}H_{172}N_4O_{24}Zn$: C 78.95, H 5.38, N 1.74. Found: C 79.06, H 5.57, N 1.62.

Zn[G−3]$_4$ P. This was prepared as above from zinc tetrakis(3,5-dihydroxyphenyl)porphine and [G−2]Br, yield 68%. UV/vis abs (ϵ) 428 nm (534 000), 518 nm (6000), 560 nm (20 000), 600 nm (7000). ^{1}H NMR δ 8.96 (s, 8 H, β-*H*); 7.48 (s, 8 H, Ar−*H*); 7.17 (m, 160 H, Ph−*H*); 7.03 (s, 4 H, Ar−*H*); 6.67 (d, 16 H, Ar−*H*); 6.53 (d, 32 H, Ar−*H*); 6.43 (t, 8 H, Ar−*H*); 6.39 (t, 16 H, Ar−*H*); 5.06 (s, 16 H, Bn−*H*); 4.83 (s, 32 H, Bn−*H*); 4.78 (s, 64 H, Bn−*H*). ^{13}C NMR δ 160.08, 160.00, 157.75 (Ar *C*−O); 149.79 (α *C*); 139.25, 139.16 (Ar *C*−CH_2); 136.62 (Ph *C*−CH_2); 128.40, 127.81, 127.40 (Ph *C*−H); 120.67, 106.57, 106.25, 101.65, 101.52, 96.67 (Ar *C*−H); 69.89 (Ar/Ph−*C*H_2). Mass spectrum (MALDI-TOF) *m*/*z* calculated 6621.1; found 6630.7. Anal. Calcd for $C_{436}H_{364}N_4O_{56}Zn$: C 79.09, H 5.54, N 0.85. Found: C 78.98, H 5.96, N 0.40.

Zn[G−4]$_4$ P. This was prepared as above from zinc tetrakis(3,5-dihydroxyphenyl)porphine and [G−3]Br, yield 20%. UV/vis abs (ϵ) 430 nm (463 000), 560 nm (21 000), 600 nm (7000). ^{1}H NMR δ 9.00 (s, 8 H, β-*H*); 7.48 (s, 8 H, Ar−*H*); 7.19 (m, 320 H, Ph−*H*); 6.67 (s, 4 H, Ar−*H*); 6.52−6.38 (overlapping resonances, 168 H, Ar−*H*); 4.91 (s, 16 H, Bn−*H*); 4.75−4.69 (overlapping resonances, 224 H, Bn−H). ^{13}C NMR δ 160.03, 159.90, 159.86, 157.76 (Ar *C*−O); 149.68 (α *C*); 139.16, 139.08 (Ar *C*−CH_2); 136.62 (Ph *C*−CH_2); 132.10 (β *C*); 128.40, 127.78, 127.45 (Ph *C*−H); 106.21, 101.42 (Ar *C*−H); 69.80 (Ar/Ph−*C*H_2). Mass spectrum (MALDI-TOF) *m*/*z* calculated 13 413.0; found 13 437. Anal. Calcd for $C_{884}H_{748}N_4O_{120}Zn$: C 79.16, H 5.62, N 0.42. Found: C 79.24, H 5.79, N 0.59.

Benzylviologen. 4,4′-Dipyridyl (0.891 g, 1.00 equiv) and the benzyl bromide (2.000 g, 2.05 equiv) were placed in a flask with acetonitrile. After heating to reflux, the yellow precipitate was collected and washed with cold acetonitrile (100%). ^{1}H NMR (in DMSO-d_6, 2.49 ppm) δ 9.57 (d, 4 H, pyr-*H*); 8.77 (d, 4 H, pyr-*H*); 7.63 (m, 4 H, Ph−*H*); 7.45 (m, 4 H, Ph−*H*); 7.42 (m, 2 H, Ph−*H*); 5.98 (s, 4 H, Bn-*H*). ^{13}C NMR (in DMSO-d_6, 2.49 ppm) δ 149.07 (Pyr *C*−Pyr); 145.55, 134.02 (Pyr *C*−H); 129.43, 129.17, 128.93 (Ph *C*−H); 127.17 (Ph *C*−CH_2); 63.10 Ph−*C*H_2). Anal. Calcd for $C_{24}H_{22}N_2Br_2$: C 57.85, H 4.45, N 5.62. Found: C 57.75, H 4.53, N 5.66.

Acknowledgment. Financial support of this research by the National Science Foundation (DMR-9641291) and by the MURI program of AFOSR is acknowledged with thanks.

CM970312+